AE International – Asia

Atmospheric Environment 38 (2004) 2111–2123

ATMOSPHERIC ENVIRONMENT

www.elsevier.com/locate/atmosenv

Aerosol chemical characteristics from sampling conducted on the Island of Jeju, Korea during ACE Asia

David Topping[a,*], Hugh Coe[a], Gordon McFiggans[a], Rachel Burgess[a], James Allan[a], M.R. Alfarra[b], Keith Bower[a], T.W. Choularton[a], Stefano Decesari[c], Maria Cristina Facchini[c]

[a] *UMIST, Department of Physics, Manchester, UK*
[b] *UMIST, Department of Chemical Engineering, Manchester, UK*
[c] *Instituto di Scienze dell'Atmosfera e del Clima , CNR, Bologna, Italy*

Received 24 September 2003; accepted 19 January 2004

Abstract

This paper presents results of an aerosol chemical characterisation experiment conducted on the Island of Jeju, Korea, using a range of techniques for analysing inorganic and organic particle components. Sulphate and ammonium were biased toward the accumulation mode size ranges. Nitrate, sodium, calcium and chloride were found in the larger size ranges and attributed to the collection of modified sea salt and dust particles. In the super-micron aerosol it was apparent that chloride depletion in sea salt had occurred which was mainly by nitrate due to reaction with nitric acid. Similarly, enhanced nitrate was found on the dust aerosol. Results derived from an aerodyne aerosol mass spectrometer (AMS) showed that sub-micron component distributions were consistent throughout the entire campaign, a lack of sub-100 nm mass loadings substantiating the notion of an aged sub-micron aerosol population. Sulphate and organic constituents were the dominant mass contributors in this size range. Various aerosol characteristics were dependent on the air mass history, the relative dominance of sulphate and organic mass loadings in the sub-micron aerosol being particularly sensitive to different air types. Loadings of organic components analysed by the AMS were found to increase significantly during direct influence from Korea. Comparison between organic components analysed by the AMS, water-soluble organic carbon (WSOC) derived from impactor sampling and organic carbon derived from a low volume sampler suggested that the volatile components analysed by the AMS were not only water soluble, but also representative of the total organic carbon present. Analysis of mass closure on impactor substrates suggested that the accumulation mode aerosol mass (200–500 nm) could be accounted for by the analysed inorganic components and WSOC. This was not found in larger size ranges, which is expected given the influence of dust and other possible non-refractory primary emissions on the measurement site.

Keywords: ACE Asia; Berner Impactor; Aerosol mass spectrometer; Aerosol chemistry; Organics

1. Introduction

The following paper presents results on aerosols sampled during the ACE ASIA campaign, on the Island of Jeju, Korea (http://saga.pmel.noaa.gov/ACEasia/).

The analysed inorganic components contributed between 18% and 38% of the total aerosol mass. These included, Na^+, NH_4^+, K^+, Mg^{2+}, Ca^{2+}, Cl^-, NO_3^- and SO_4^{2-} derived from impactor sampling and NO_3^-, SO_4^{2-} and NH_4^+ provided by an aerosol mass spectrometer (AMS). Organic compounds were also analysed as water-soluble organic carbon (WSOC) derived from impactor sampling and organic constituents analysed by the AMS. Numerous studies have suggested that organic

*Corresponding author. Fax: +44-161-200-3651.
E-mail address: david.topping@postgrad.umist.ac.uk (D. Topping).

1352-2310/$ - see front matter © 2004 Elsevier Ltd. All rights reserved.
doi:10.1016/j.atmosenv.2004.01.022

components comprise a significant proportion of the aerosol mass (e.g. Saxena and Hildemann, 1996 and citations therein; Krivacsy et al., 2001) and that WSOC may constitute a significant fraction of particulate organic matter (e.g. Zappoli et al., 1999). On average, the contribution of WSOC was found to range from 6.5% to 31% of the total aerosol mass.

Sampling was conducted on the western edge of Jeju island, in the Gosan district (see Carmichael et al., 1996). Jeju is a major resort with no large industrial sources (Carmichael et al., 1997) and as such is an ideal location to monitor the chemistry of East Asia. Numerous aerosol characterisation studies have been carried out, both at Jeju (Carmichael et al., 1996, 1997; Chen et al., 1997; Kim et al., 2002), and in surrounding areas (Mukai et al., 1990; Matsumoto et al., 1998).These have generally highlighted specific trends of aerosol loadings and characteristics that are largely dependent on the air mass history. Indeed, the study site is well known for its favourable geographical location for studying various aspects of diverse source regions that are best reflected by relatively systematic wind patterns (Kim et al., 2002). Winter, spring and autumn are dominated by continental outflows, with winter and autumn under the influence of northwesterly trajectories and spring under westerly flows. Typical trajectories experienced during ACE ASIA are given in Fig. 1 along with the dates on which they occurred. The back trajectories were calculated using the HYSPLIT on-line transport and dispersion model (Draxler and Rolph, 2003).

Northern China is the second largest source of atmospheric dust in the world (Xuan and Sokolik, 2002) and given that dust storms advecting off the Asian continent are likely to interact with polluted boundary layers before reaching Jeju, the propensity of dust storms occurring in East Asia has implications regarding the nature of particulate matter residing there. There is a large body of observational data that suggests mineral aerosols are an important reactive surface globally (e.g. Dentener et al., 1996) and the state of aged dust aerosols in East Asia has been studied and reported in the past (e.g. Fan et al., 1996; Chen et al., 1997).

Relative humidity was high across the whole campaign, with a mean of 77% and a standard deviation of 13%. The average temperature was found to be 16°C (standard deviation of 3°C). Wind speed was also high on numerous occasions yet rarely increased above $12\,ms^{-1}$ (average of $6.2\,ms^{-1}$).

2. Sampling and analysis

Forty aerosol samples taken with a 5-stage Berner impactor (Berner and Lurzer, 1980) were collected during the ACE ASIA experiment from 13 to 29 April 2001. The impactor allowed aerosol collection onto four stages equipped with tedlar substrates, and onto a Teflon back filter. The cut offs for each stage were: $<0.2\,\mu m$ (Base filter); 0.2–0.5 μm (Stage 1); 0.5–1.5 μm (Stage 2); 1.5–5.5 μm (Stage 3); 5.5–10 μm (Stage 4). The concentrations of inorganic ions (Na^+, NH_4^+, K^+, Mg^{2+}, Ca^{2+}, Cl^-, NO_3^-, SO_4^{2-}) and low-molecular weight organic acids (acetate, formate, MSA and oxalate) were determined by ion chromatography (IC). A Dionex 4500 instrument equipped with a CS12A column and a Dionex 500 instrument with an AS11 column (Dionex) were used for the analysis of cations and anions, respectively. The WSOC was determined using a total organic carbon analyser (Shimadzu TOC-5000A). A new technique proposed by Decesari et al. (2000a), also allowed a more detailed organic characterisation of the major WSOC contributory species to be made, the results of which will be presented in a future publication.

Aerosol sampling was also carried out using an Aerodyne aerosol mass-spectrometer at Jeju (hereafter referred to as the AMS), which provides mass loadings of the volatile and semi-volatile aerosol components as a function of particle size. Details regarding the operation and calibration of the instrument can be found in the literature (Allan et al., 2003a, b; Jimenez et al., 2002). The AMS samples particles with near 100% efficiency in the size range from 70 to 700 nm aerodynamic diameter and the following report presents results regarding sulphate, nitrate, ammonium and organic mass loadings. The organic mass obtained from the AMS is the total mass of the organic fraction, not the mass of carbon within the fraction.

3. Results and discussion

3.1. Impactor data

Total average loadings (PM10) found during ACE ASIA are presented in Table 1, along with the maximum, minimum and standard deviations. Ammonium, potassium and calcium loadings were similar to the annual average found by Carmichael et al., 1996 and Chen et al. (1997) ($NH_4^+ = 1.4\,\mu g\,m^{-3}$; $K^+ = 0.4\,\mu g\,m^{-3}$; $Ca^{2+} = 0.5\,\mu g\,m^{-3}$; $Na^+ = 1.7\,\mu g\,m^{-3}$; $Cl^- = 1.9\,\mu g\,m^{-3}$). Comparatively lower loadings of sodium and chloride can be explained by the low wind speeds during ACE ASIA, as sea-salt particles are noted to be more prevalent during winter periods when wind speeds are higher (Chen et al., 1997). However, the $[Na^+]$ to $[Cl^-]$ ratio was also high due to chloride depletion mechanisms, most likely linked to high NO_x concentrations in northerly flows. The relatively high standard deviations of each component reflect the multitude of air mass types affecting Jeju. Loadings presented here were found

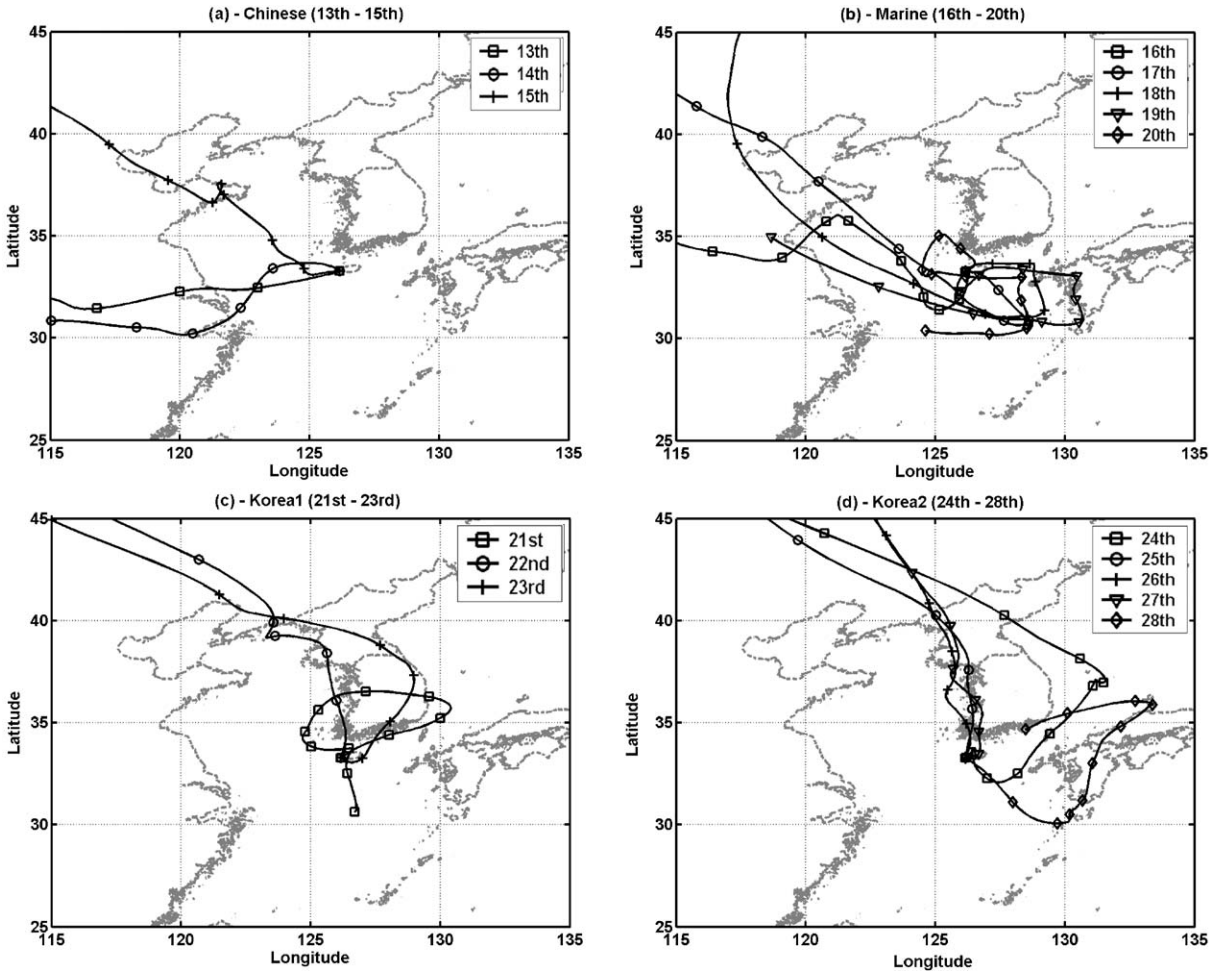

Fig. 1. 5 day back trajectories for selected regimes: (a) Chinese regime (13–15 April 2001). (b) Marine regime (16–20 April 2001). (c) First Korean regime (21–23 April 2001). (d) Second Korean regime (24–28 April 2001). Tagged at 12 h intervals.

Table 1
Average PM10 concentrations of IC analysed components for the whole campaign (in $\mu g\,m^{-3}$)

	Na	NH_4	K	Mg	Ca	SO_4	NO_3	Cl	Acetate	Formate	Oxalate	MSA	WSOC
Average	0.54	1.32	0.28	0.27	0.30	3.58	1.40	0.39	0.11	0.10	0.43	0.35	6.71
Maximum	1.48	2.74	0.94	1.17	1.16	8.81	3.99	0.95	0.28	0.29	1.13	1.25	16.31
Minimum	0.00	0.00	0.00	0.00	0.00	0.00	0.00	0.00	0.00	0.00	0.00	0.00	0.00
S.D.	*0.35*	*0.66*	*0.19*	*0.27*	*0.28*	*1.90*	*0.99*	*0.29*	*0.06*	*0.07*	*0.29*	*0.29*	*3.62*

to be larger than those presented by Matsumoto et al. (1998), who collected samples from December 1994 to January 1997 on the Ogasawara islands, in the Sea of Japan ($nssSO_4^{2-} = 1.75\,\mu gm^{-3}$; $NO_3^- = 0.592\,\mu g\,m^{-3}$; $NH_4^+ = 0.251\,\mu g\,m^{-3}$; $Cl^- = 6.13\,\mu g\,m^{-3}$; $Na^+ = 4.31\,\mu g\,m^{-3}$; $Ca^{2+} = 0.375\,\mu g\,m^{-3}$) and considerably larger than nitrate and sulphate loadings collected over the remote Pacific presented by Savoie and Prospero (1989a, b). Similarly, lower concentrations were found by Mukai et al. (1990), who analysed monthly filters taken at Oki Island, Japan, roughly 700 km northeast of Jeju ($SO_4^{2-} = 3.59\,\mu g\,m^{-3}$; $NH_4^+ = 0.51\,\mu g\,m^{-3}$; $Na^+ = 0.43\,\mu g\,m^{-3}$; $NO_3^- = 0.114\,\mu g\,m^{-3}$; $Cl^- = 0.046\,\mu g\,m^{-3}$; $Ca^{2+} = 0.151\,\mu g\,m^{-3}$). The contribution from WSOC analysed during ACE ASIA

was important. Indeed, concentrations were found to increase to levels as high as 18.2 $\mu g m^{-3}$, and average concentrations were the highest of all analysed components.

3.2. AMS data

Mass trends of components analysed by the AMS are shown in Fig. 2. Results indicate that sulphate and organic components were clearly more abundant relative to nitrate and ammonium mass loadings, and that both were particularly variable. Such data are very useful and help to define sampling regimes with different air mass histories. The two most pronounced results are the increase in sulphate to 14 $\mu g m^{-3}$ during an aged marine period, and the increase in organic loadings, again reaching around 14 $\mu g m^{-3}$, during the second Korean period.

Fig. 2(d) shows the size distributions of analysed components derived from AMS measurements, averaged across different back trajectory regimes. Table 4 presents averaged mass loadings from the AMS, across the 70–700 nm size range, for the different trajectory classifications defined in Fig. 1. A discussion of the size dependent sampling efficiencies and various other constraints of the AMS can be found in the literature (Allan et al., 2003a, b). Distributions were found to be consistent. Indeed, the shape of the size distribution of sulphate was found to be relatively constant from day to day, in agreement with aircraft measurements taken by Bahreini et al. (2003). As shown in Table 4, sulphate and organic components were the dominant contributors to AMS mass loadings across the whole campaign. Organic components were found to be higher than those of nitrate, and indeed slightly higher than sulphate, with a summed mass loading of 3.49 $\mu g m^{-3}$ across the 70–700 nm size range. Ammonium loadings in the sub-micron range were low in contrast to sulphate and organic constituents (1.48 $\mu g m^{-3}$). An important observation was that nitrate concentrations were found to be persistently negligible in the sub-micron mode, relative to sulphate and organic components, and tended to be present in larger size ranges. However, deriving any quantitative conclusions regarding super-micron size distributions of AMS components is not possible with the inlet system that was operated during ACE ASIA. Another interesting observation, from the AMS, was that nitrate was found to be more variable than sulphate in the accumulation mode. The sub-micron nitrate was found to vary according to back trajectories, which is treated separately later, and one might expect that it is only present in younger air masses. The contribution from organic components was found to be variable in mass loading. Interestingly, concentrations were found to increase substantially during influence from the Korean mainland.

A discussion of composition variations according to different back trajectory regimes is now given.

Tables 2 and 3 give the average concentrations and average fractional molar contributions from the analysed components, according to different back trajectory regimes, respectively.

3.3. Chinese outflow

During the period 13–15 April 2001, air masses arriving at Jeju had advected off the Chinese mainland within the last two days before measurement (Fig. 1a). Pronounced results include highest average loadings and a clear dominance of sulphate toward sub-micron loadings sampled by the AMS. Strongest relations were found between impactor nss-sulphate and ammonium, particularly on stage 1 ($R = 0.94$) which seemed to be composed mainly of these two components throughout the campaign. Fig. 3a shows the molar ratios of the sulphate and ammonium on this impactor stage. The majority of data points suggest that particles in this size range were predominantly composed of ammonium sulphate, within the derived experimental uncertainty. However, for the single Chinese outflow sample, there is apparently insufficient ammonium to fully neutralise the available sulphate. Although represented by a single data point, this may be due to the high sulphur emissions over the industrialised regions of China matched by lower ammonia emissions.

The most interesting result from this period was the clear influence from dust particles. Highest loadings of Ca^{2+} were found during this period, with 1.03 $\mu g m^{-3}$ on stage 3 (1.5–5.5 μm) and 0.43 $\mu g m^{-3}$ on stage 4 (5.5–10 μm). Sulphate loadings were slightly higher on stage 3 with respect to the remaining sampling period but the most pronounced effect was the increase in nitrate on stage 3 (1.5–5.5 μm). Chloride depletion was found to be 20% during this period. Given this and the fact that ammonium loadings were low (0.08 $\mu g m^{-3}$), in contrast to nss-sulphate and nitrate, it is possible that the observed increase of the two anions was associated with dust particles. On stage 4 however (1.5–10 μm), chloride depletion was 41.9% and it is possible that sulphate and nitrate deposited on sea-salt particles as well as dust aerosols. Luria and Sievering (1991) suggest that SO_2 reactions on sea-salt aerosol are likely to be more important. A relatively high correlation was found on stage 1 between nitrate and ammonium (0.56). In addition, larger correlations were found between nitrate, ammonium and the crustal components calcium, potassium, magnesium and sodium on stages 3 and 4 than those between nss-sulphate and these components. Hence, it is likely that nitrate was enriched in dust or sea-salt particles, rather than being associated with ammonium. Previous studies have reported that particulate sulphate and nitrate displace more volatile

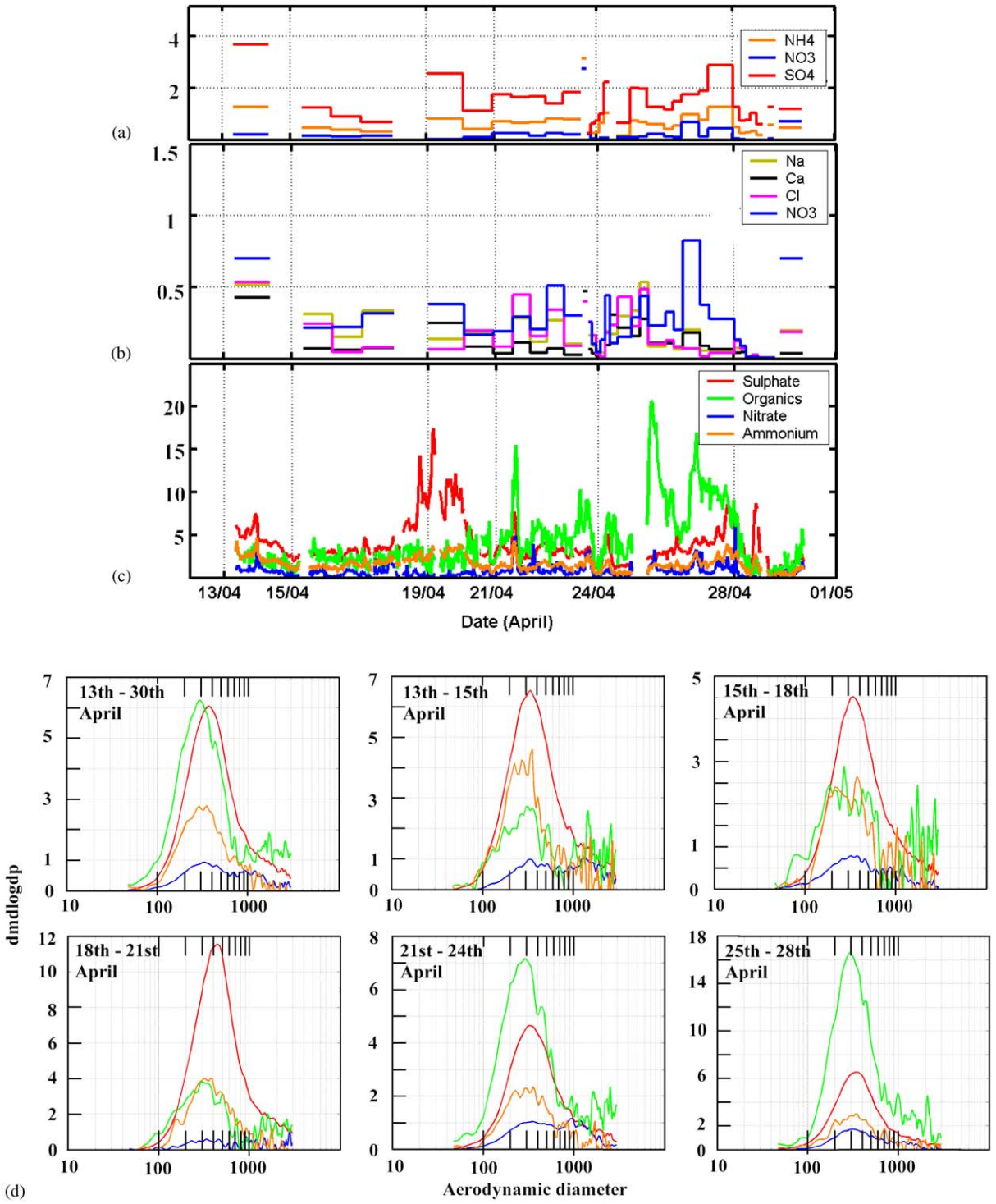

Fig. 2. (a) Impactor mass time trends for stage 1 (0.2–0.5 μm). (b) Impactor mass time trends for stage 4 (5.5–10 μm). (c) Total summed AMS mass loadings across the whole campaign. (d) Average size distributions for analysed AMS components across specific dates (size in nanometres). Loadings are in $\mu g\,m^{-3}$.

Table 2
Average concentrations, in nanomoles per cubic metre, according to the back trajectory regimes defined in Fig. 1

Regime	Size range (μm)	Na	NH_4	K	Mg	Ca	SO_4	NO_3	Cl	Ac	For	O_x	MSA
Whole	0.2–0.5	4.54	35.80	2.62	0.25	0.93	16.72	3.96	1.20	0.67	0.48	0.63	0.26
Campaign	0.5–1.5	10.40	30.36	3.35	1.27	3.10	16.39	9.42	4.18	0.66	0.73	0.56	0.14
	1.5–5.5	14.26	8.65	1.72	1.66	5.08	5.88	12.15	7.70	0.42	0.48	0.23	0.05
	5.5–10	8.97	7.39	1.33	0.69	2.57	4.53	5.34	4.52	0.40	0.29	0.14	0.07
	Total	**38.17**	**82.20**	**9.03**	**3.88**	**11.69**	**43.52**	**30.87**	**17.60**	**2.15**	**1.98**	**1.56**	**0.51**
Chinese	0.2–0.5	2.43	69.68	5.50	0.16	1.71	38.12	3.37	0.50	0.35	0.58	0.77	0.44
	0.5–1.5	16.17	49.34	10.78	3.88	10.51	32.94	23.72	10.55	0.56	2.88	1.01	0.54
	1.5–5.5	31.51	4.37	3.71	5.75	25.59	12.18	41.62	29.23	0.07	2.95	0.28	0.48
	5.5–10	22.44	1.05	1.45	1.87	10.63	9.84	11.13	15.16	0.57	0.68	0.09	0.51
	Total	**72.55**	**124.44**	**21.44**	**11.66**	**48.44**	**93.08**	**79.84**	**55.44**	**1.55**	**7.09**	**2.15**	**1.97**
Marine	0.2–0.5	3.04	26.20	3.05	0.04	0.47	13.53	1.70	0.64	0.34	0.20	0.31	0.28
	0.5–1.5	13.21	33.54	5.01	1.38	2.99	21.92	7.17	3.87	0.81	0.16	0.56	0.34
	1.5–5.5	16.98	2.69	1.11	1.90	6.10	8.24	11.73	6.46	0.31	0.23	0.13	0.10
	5.5–10	9.79	1.72	0.56	0.69	2.71	3.82	4.13	3.56	0.38	0.14	0.06	0.19
	Total	**43.03**	**64.14**	**9.73**	**4.02**	**12.28**	**47.52**	**24.73**	**14.53**	**1.83**	**0.73**	**1.06**	**0.91**
Korean	0.2–0.5	6.08	39.91	3.23	0.29	1.25	18.03	4.69	1.26	0.91	0.66	0.73	0.30
	0.5–1.5	12.73	26.34	3.63	1.53	3.74	13.59	11.33	5.10	0.78	0.91	0.55	0.09
	1.5–5.5	18.01	11.22	2.32	2.06	5.91	6.35	14.69	9.59	0.60	0.56	0.29	0.00
	5.5–10	11.02	9.54	1.92	0.83	3.08	5.20	6.30	5.57	0.51	0.31	0.16	0.01
	Total	**47.84**	**87.00**	**11.09**	**4.71**	**13.98**	**43.18**	**37.01**	**21.53**	**2.80**	**2.45**	**1.74**	**0.40**

Table 3
Average fractional molar contributions, according to the back trajectory regimes defined in Fig. 1

Regime	Size range (μm)	Na	NH_4	K	Mg	Ca	SO_4	NO_3	Cl	Acetate	Formate	Oxalate	MSA
Whole	0.2–0.5	0.0667	**0.5256**	0.0385	0.0037	0.0137	**0.2455**	0.0581	0.0176	0.0098	0.0071	0.0092	0.0038
Campaign	0.5–1.5	**0.1288**	**0.3761**	0.0415	0.0158	0.0384	**0.2031**	**0.1167**	0.0518	0.0082	0.0090	0.0070	0.0017
	1.5–5.5	**0.2444**	**0.1482**	0.0295	0.0284	0.0871	**0.1007**	**0.2083**	**0.1319**	0.0072	0.0082	0.0040	0.0008
	5.5–10	**0.2462**	**0.2030**	0.0366	0.0189	0.0706	**0.1244**	**0.1467**	**0.1242**	0.0111	0.0079	0.0037	0.0018
Chinese	0.2–0.5	0.0197	**0.5636**	0.0445	0.0013	0.0138	**0.3083**	0.0273	0.0040	0.0028	0.0047	0.0062	0.0036
	0.5–1.5	0.0993	**0.3029**	0.0662	0.0238	0.0645	**0.2022**	**0.1456**	0.0648	0.0034	0.0177	0.0062	0.0033
	1.5–5.5	**0.1997**	0.0277	0.0235	0.0364	**0.1622**	0.0772	**0.2638**	**0.1853**	0.0004	0.0187	0.0018	0.0030
	5.5–10	**0.2973**	0.0139	0.0192	0.0248	**0.1408**	**0.1304**	**0.1475**	**0.2008**	0.0076	0.0090	0.0012	0.0068
Marine	0.2–0.5	0.0611	**0.5259**	0.0612	0.0008	0.0094	**0.2717**	0.0342	0.0129	0.0067	0.0040	0.0063	0.0057
	0.5–1.5	**0.1451**	**0.3684**	0.0550	0.0152	0.0328	**0.2408**	0.0788	0.0425	0.0089	0.0018	0.0061	0.0038
	1.5–5.5	**0.3031**	0.0479	0.0199	0.0339	**0.1089**	**0.1470**	**0.2092**	**0.1152**	0.0055	0.0041	0.0024	0.0018
	5.5–10	**0.3519**	0.0618	0.0202	0.0249	0.0975	**0.1374**	**0.1484**	**0.1280**	0.0135	0.0050	0.0021	0.0068
Korean	0.2–0.5	0.0786	**0.5155**	0.0417	0.0038	0.0161	**0.2329**	0.0606	0.0163	0.0117	0.0086	0.0095	0.0038
	0.5–1.5	**0.1581**	**0.3271**	0.0451	0.0189	0.0465	**0.1688**	**0.1406**	0.0633	0.0097	0.0113	0.0069	0.0012
	1.5–5.5	**0.2512**	**0.1565**	0.0323	0.0287	0.0824	0.0886	**0.2049**	**0.1338**	0.0084	0.0078	0.0040	0.0000
	5.5–10	**0.2465**	**0.2133**	0.0429	0.0186	0.0689	**0.1163**	**0.1410**	**0.1247**	0.0114	0.0070	0.0037	0.0003

inorganic components in this region of the globe (hydrochloric acid in the case of sea-salt aerosol and carbonate/bicarbonate in the case of mineral aerosol) during the aging process (Fan et al., 1996; Song and Carmichael, 1999). This combined with data regarding the composition of Asian dust (Nishikawa, 1993; Zhang and Iwasaka, 1999) implies that dust had evolved before arriving at Jeju. The dominance of nitrate, rather than sulphate, assumed to be associated with dust here is supported by the laboratory studies of Hanisch and

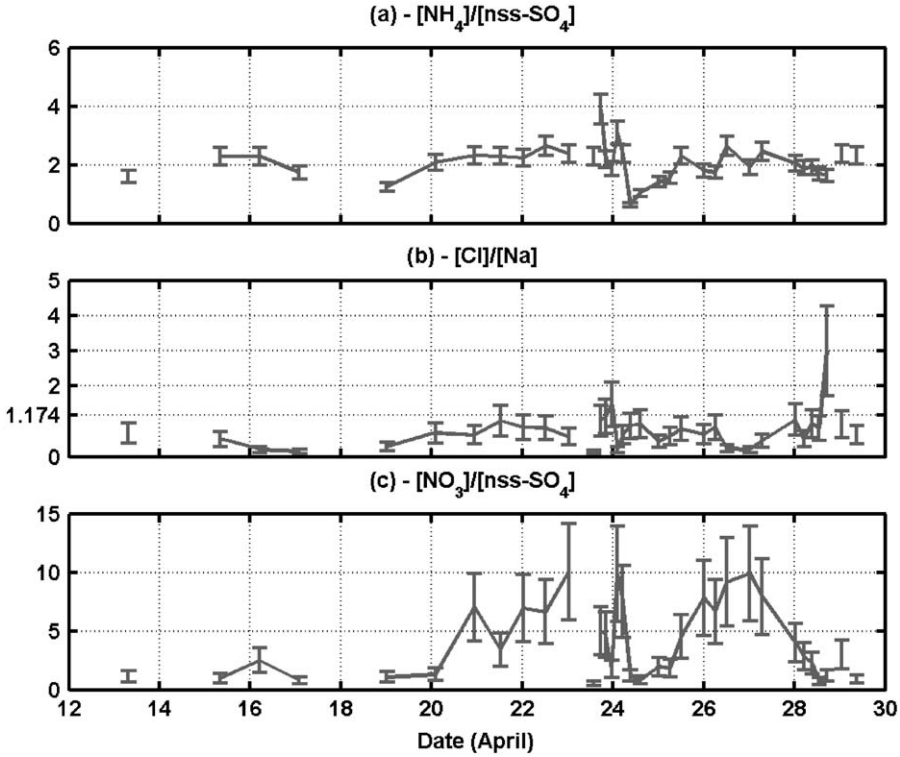

Fig. 3. (a) Molar ratios of NH_4^+ to nss-SO_4^{2-} in the 0.2–0.5 μm range. (b) Molar ratios of Cl to Na in the 1.5–5.5 μm size range. Points below a ratio of 1.174 indicate chloride deficiency. (c) Molar ratios of NO_3^- to nss-SO_4^{2-} in the 5.5–10 μm size range.

Crowley (2001a, b), who found that a large and irreversible uptake was observed between HNO_3^- and various authentic dust samples (including samples from Chinese dust regions).

3.4. Marine influenced air

During the period 16–20 of April, air masses arriving at Jeju had spent between 2 and 5 days prior over the Yellow Sea and areas west of Kyushu Island (Fig. 1b). Table 2 shows that averaged component loadings were smaller than those found during the initial Chinese outflow, yet comparable to those found during both Korean periods. During 17th–19th, air masses arriving at Jeju had spent 5 days over oceanic regions around Jeju, and areas in close proximity to Kyushu Island. On the 19th, after spending 5 days over oceanic regions, the third travelling over the western edge of Kyushu Island, loadings of various components were very high, those being Mg^{2+}, K^+, NO_3^-, Ca^{2+}, SO_4^{2-}, and NH_4^+. Higher loadings of sulphate and ammonium were found in the 0.5–1.5 μm size range than those found during the initial Chinese outflow (Table 2). Whilst there was some evidence of linear correlation between MSA and nss-sulphate in the 0.2–1.5 μm range ($R=0.63$ for stage 1 and 0.69 for stage 2), the [MSA]: [nss-SO_4^{2-}] ratios were found to be at least a factor of 5 below the relationship derived by Savoie and Prospero (1994), and supported by Arimoto et al. (1996), for the contribution of DMS oxidation to nss-SO_4^{2-} production. Fig. 2(c) shows that total AMS mass loadings were found to be variable during this "marine" period. During 18th and 19th, the contribution from sulphate clearly increases as air mass back trajectories indicate influence from marine areas and Kyushu Island. Average total sulphate loadings, derived from the AMS, increased to 5.33 from 2.42 $\mu g\,m^{-3}$ (Table 4), the remaining three components maintaining loadings similar to the early stages of this marine period. If one looks at the 18th and including the 19th, the most pronounced effect is the clear dominance of sulphate to the analysed AMS constituents of the sub-micron aerosol. Loadings of WSOC dropped during this period, relative to the initial Chinese outflow. Chloride depletion was high here, ranging from 62% to 93% on stage 3 and 57% to 87% on stage 4 and attempts to achieve closure here indicated that nitrate could not account for the chloride loss alone. Indeed, the contribution from nss-sulphate during this period was significant, whereas during the remainder of the campaign its contribution deemed secondary to that of nitrate. This pronounced effect of sulphate interaction is interesting and the study of Chameides and Stelson

Table 4
Averaged summed AMS mass loadings in the 70–700 nm size range. Results are partitioned into different time periods, defined using back trajectory regimes in the text. Loadings are in $\mu g m^{-3}$

		Date					
		13–15	15–18	18–21	21–24	25–28	13–30
SO_4	Mean	3.56	2.42	5.33	2.52	3.37	3.09
	Max	6.02	3.7	14.48	5.8	7.17	11.45
	S.D.	0.98	0.43	2.69	0.82	1.21	1.74
NH_4	Mean	2.14	1.33	1.92	1.3	1.55	1.48
	Max	8.47	17.24	4.25	5	7.18	17.24
	S.D.	2.42	2.12	1.13	0.77	0.94	1.45
NO_3	Mean	0.49	0.46	0.29	0.65	0.88	0.51
	Max	2.49	1.98	1	3.43	4.82	4.82
	S.D.	0.4	0.41	0.26	0.63	0.69	0.55
Organic	Mean	1.5	1.65	2.17	4.14	8.35	3.49
	Max	3.9	4.95	6.08	12.44	15.95	15.95
	S.D.	0.87	1.51	1.4	2.06	2.86	3.14

(1992) suggested that sea salt may remove a significant amount of sulphur from the marine atmosphere and thereby suppress the SO_2 concentrations in the marine boundary layer. Sievering et al. (1991) found that oxidation of SO_2 by O_3 proceeds rapidly in freshly formed coarse sea-salt particles when they contained water and suggest this to be the major pathway for the formation of coarse mode nss-sulphate in the marine boundary layer.

3.5. Korean influenced air

During periods 21–23 and the 25–27, air trajectories changed from north westerly to northerly, with air masses now advecting across from the Korean mainland (Figs. 1c and d). Whilst component concentrations differed little from the aged marine period (Table 2), one can see that, compared to the other regimes, nitrate was particularly more abundant in the coarse mode during both of the Korean periods. This is most likely linked with an increase in source strength of nitrate precursors. Chloride loadings increased drastically during this period, whereas sodium loadings remained relatively constant, the highest found on impactor stage 3 (1.5–5.5 μm). The molar ratios of ammonium to sulphate in the accumulation mode shown in Fig. 3(a) indicate that, during this first Korean period, there was evidently enough ammonium to fully neutralise the available sulphate on stage 1, leading to the suggestion that accumulation mode aerosols were composed of ammonium sulphate here. This is probably linked to higher ammonia emissions over new source regions of mainland Korea, and also raises the possibility of ammonium nitrate aerosols in the accumulation mode. The second Korean period, defined as 25–27 of April, encompassed what was thought to be another dust event, as witnessed by increased loadings of Ca^{2+} on stages 2–4 (1.5–10 μm), with a maximum on stage 3 (around 18 $nmol m^{-3}$). Levels of NH_4^+ and SO_4^{2+} appear to be unaffected by this process. Loadings of NO_3^- increase relative to the short marine period, although not to an extent observed during the initial Chinese outflow. Again, sulphate levels were unaffected by this event on stages 3 and 4 (1.5–10 μm), suggesting little interaction between dust particles and gaseous sulphur compounds. In addition, the accumulation mode aerosols (0.2–0.5 μm) seemed to be composed mainly of ammonium sulphate again, as during the first Korean period. Size distributions obtained from the AMS were separated into the two different Korean outflows (Fig. 2d). It is interesting to note that during both outflows, the contribution from organic components increased relative to the previous regimes, particularly during the second outflow. Similarly the contribution from sulphate decreased relative to the aged marine outflow, but was comparable to that found during the Chinese outflow period. Table 4 shows that average total loadings (70–700 nm) from the AMS increased during the second Korean period, relative to the first. Again, the most pronounced increase was that of average organic mass loadings from 4.91 to 8.35 $\mu g m^{-3}$

3.6. Sensitivity studies

3.6.1. Mass closure

Comparisons between IC, organic analysis, and gravimetric loadings were made in order to assess the extent of mass closure during ACE ASIA. As shown in

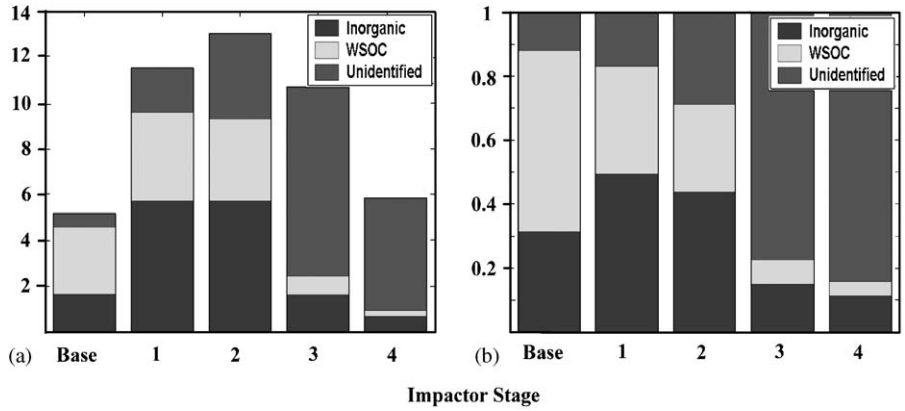

Fig. 4. (a) Average analysed and gravimetric mass loadings for the whole campaign ($\mu g\,m^{-3}$). (b) Average mass fractional contributions for each impactor stage, for the whole campaign.

Fig. 4, it was found that the fraction of unidentified mass increased with size. In the smaller sizes, an important contribution to the mass can be due to water-insoluble organic carbon (WIOC) and black carbon not determined by the analytical protocol. The contributions from both WSOC and inorganic mass were found to be larger in the smaller size ranges. Indeed, both were found to account for 34% and 49% of the mass on stage 1 (0.2–0.5 μm) with a smaller 4% and 11% found on stage 4 (5.5–10 μm). It is suggested that aerosols within the 0.2–0.5 μm size range are therefore largely characterised by inorganic components and WSOC only. It is clear that aerosols within larger size ranges could not be characterised by WSOC and inorganic components alone, but contain insoluble crustal components, which have not been analysed.

3.6.2. AMS vs. impactor intercomparison

The loadings of components analysed by the AMS were compared with those derived from impactor samples within the 200–500 nm (0.2–0.5 μm) size range. Such a size range was chosen to include the region in which the AMS samples aerosols with near 100% efficiency, and also encompass a single impactor sampling size range. Correlation coefficients and mean differences between the two datasets are given in Table 5. The correlation coefficients and ratios found for sulphate and ammonium suggest a good relationship between these components. A high correlation was found for nitrate, yet the average ratio indicates that the AMS recorded roughly 70% of the impactor derived loading. The comparison between the AMS organics and WSOC derived from the impactor indicates a high correlation and mean ratio between the two, with a ratio similar to that found for sulphate and ammonium.

Table 5
Comparison between the AMS and impactor analyses given by the correlation coefficients (R) and average ratios between the two datasets (AMS/impactor loadings)

	Sulphate	Nitrate	Ammonium	Organics
R	0.52	0.79	0.44	0.87
Ratio	1.44	0.702	1.06	1.05

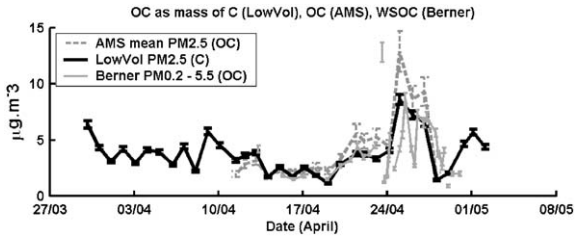

Fig. 5. Comparison between OC derived from a LowVol sampler (PM2.5), WSOC derived from a Berner impactor (PM 1.5, PM5.5) and organic components derived from AMS measurements averaged to the same time frame as the LowVol sampler. Results are also given for the Berner PM data calculated without the contribution from the base filter, the validity of which is discussed in the text.

Organic analyses:

Fig. 5 shows the temporal comparison between the AMS derived volatile organic components (in mass of OC), WSOC from impactor sampling (in mass of OC) and OC derived from a low volume (LowVol) sampler using the method described by (Mader et al., 2003) presented as mass of C. The base filters of the Berner impactor were not included in this analysis. During the Korean period, it was found that the base filter contributed over half of the WSOC mass loadings

implying an extremely large number of small particles that were not observed and the AMS measurements do not show a significant sub 200 nm mass mode. The choice of PM5.5 concentrations from the Berner impactor was chosen to enclose the 2.5 μm boundary within the size cut of stage 1 (1.5–5.5 μm) as most of the WSOC was found in the accumulation mode.

There is good temporal agreement between the datasets even though the three different techniques have different operational definitions of organic carbon. It is on other hand clear from the impactor mass balance, that in the fine fraction, approximately 20% of the mass is unidentified that could be attributed to insoluble carbonaceous material. For a review of different analytical methods for OC, the reader is referred to the literature (Jacobson et al., 2000). Kim et al. (2000) found that the PM2.5 EC/OC ratio at Gosan spanned from 2% to 10%, and therefore it is possible that EC could have influenced loadings. Generally, the AMS organic derived components were slightly higher than total organic carbon, but as the AMS measures total organic mass, not the carbon mass in the organic fraction as discussed earlier, this is not surprising and correlation coefficients combined with the above discussion emphasise the good agreement between the two. The analysis can be taken further by analysing conversion factors required to equate the different organic loadings. To do this, two calculations must be carried out. The first is the conversion of water-soluble organic loadings to mass of C using the scaling factor of 1.9. Second, the WSOC data from the impactor was linearly interpolated onto the common time base of the AMS and LowVol organic data. Subtracting the WSOC carbon mass from the LowVol carbon mass leaves the water insoluble fraction sampled by the LowVol impactor. This fraction can then be added to the interpolated mass of water-soluble organic material and scaled to match with the AMS derived mass loadings. The scaling factor required, along with common conversion factors used to convert non-WSOC carbon loadings to organic mass loadings in the literature, can then be used to analyse the agreement between the data sets. An average scaling factor of 1.07 was found for the ACE ASIA data set implying that the non-WSOC had a low conversion factor. However, when one includes error propagation analysis, the average difference ranged from 1.6 to 0.5. Taking the study of Matta et al. (2001), one might use mass conversion factors of around 1.4 and 1.0 for WIOC and elemental carbon (EC), respectively. Hence, if the conversion factor used to derive WSOC loadings (1.9) was indicative of the sampled aerosols, then the AMS and LowVol organic mass loadings agree fairly well and it suggests that the AMS organic loadings were possibly representative of the total OC present. The conversion factor of 1.9 used for deriving organic mass loadings of WSOC was based on the technique of Decesari et al. (2000a) and the results regarding WSOC functionality will be presented in a future publication. The proposed chemical models for representing the composition of the three main classes of organics analysed by this technique, presented by Decesari et al. (2000b), have conversion factors of 2.0 for neutral compounds, 2.1 for mono-/di-acids and 1.7 for poly acids. The correlation coefficients and average ratio between the AMS and LowVol organic data are provided in Table 6.

Fig. 6 shows the contribution from three representative m/z fragments that contribute to the total AMS organic mass loadings, averaged across the whole campaign. Laboratory experiments showed that mass spectra obtained using the AMS compare very well to the NIST standard library of mass spectra except in the case of di- and poly carboxylic acids and humic-like substances, where m/z 44 was found to be much more pronounced in the AMS spectra. This is reproducible and the m/z 44 mass loading is proportional to the concentration of these components. Other classes of compounds show only minor peaks at $m/z = 44$, indicating that the $m/z = 44$ mass fragment can therefore be

Table 6
Correlation coefficients and ratios between the AMS derived organic loadings and OC carbon data from the LowVol sampler for different size ranges. The ratio is defined as AMS loadings divided by LowVol loadings

Size	R	Mean ratio
PM1	0.95	1.16
PM2.5	0.94	1.2
TSP (LowVol)	0.52	0.69
Total AMS		

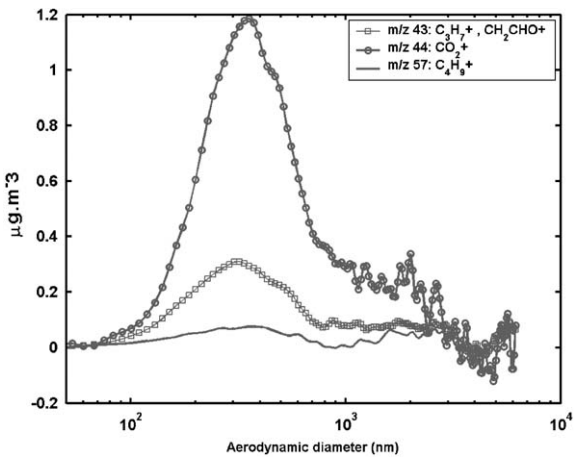

Fig. 6. Size distribution of three ion fragments representative of organic components contributing to the derived AMS organic mass, averaged across the whole campaign (see text).

used as a marker of oxidized organic compounds measured by the AMS.

The most pronounced result in Fig. 6 is the dominant contribution from m/z 44 (CO_2^+). This ion is the largest contributor to the total organic mass. The distribution is clearly unimodal, with a modal diameter of around 400 nm. The second highest contributor is m/z 43; this mass fragment typically shows bi-modal distributions in urban environments and has two main contributing ions. The first is $C_3H_7^+$, which is representative of hydrocarbon species; the second source is from CH_2CHO^+, which is indicative of oxidised organics, ketones and aldehydes. The former ion dominates at smaller sizes and in urban environments, usually residing on particles around 100 nm in size, the latter, in more aged air and in larger particle sizes (Allan et al., 2003b). The lack of m/z 43 within the smaller size ranges is again consistent with organics in aerosols sampled during ACE ASIA being aged and heavily oxidised. That m/z 57, an alkyl chain fragment ($C_4H_9^+$), was found to make a negligible contribution to the organic mass, is also consistent with this hypothesis. There are clear indications from the AMS that the organic fraction is heavily oxidised and is likely to contain carboxylic acids and/or humic-like substances at very significant concentrations. This is entirely consistent with the measurements of the functionality of the WSOC that show 60% of the WSOC is composed of di carboxylic acid and humic-like material, the results of which will be presented in a future publication.

4. Conclusion

Results regarding the chemical analysis of aerosols sampled during the ACE ASIA campaign, on the Island of Jeju, were presented using various analytical techniques. Averaged across the whole campaign, it was found that the major contributory inorganic components were sulphate, ammonium, nitrate, calcium, sodium and chloride. Sulphate and ammonium were biased toward the accumulation mode size ranges. Nitrate, sodium, calcium and chloride, however, were predominantly found in the larger size ranges and were attributed to the collection of sea-salt and dust particles, which had evolved during transport. It was found during an identified dust event that loadings of nitrate were particularly enhanced in the coarse mode, implying interactions between HNO_3 and dust particles. Analysing the contribution from nitrate and nss-sulphate to chloride loss revealed that nss-sulphate was only found to have a substantial effect during an aged marine outflow. This was probably due to the aqueous phase oxidation of anthropogenic SO_2 in cloud over the sea.

Sub-micron component distributions, derived from AMS measurements, were fairly consistent throughout the entire campaign, a lack of sub 100 nm mass loadings consistent with an aged sub-micron aerosol population. Sulphate and organic constituents were the dominant mass contributors in this size range and their relative dominance sensitive to varying air mass history. During the Chinese outflow, and specifically the aged marine period, sulphate was clearly the dominant contributor to sub-micron AMS loadings. As circulation patterns varied and northerly flows brought in air influenced by the Korean Peninsula, organic constituents became the dominant mass contributors. Indeed, results of both OC and WSOC loadings from impactor sampling indicated not only that highest loadings were found in the accumulation mode aerosol, but also such loadings increased during direct influence from the Korean mainland.

Comparison between organic components analysed by the AMS, WSOC derived from impactor sampling and OC derived from a LowVol sampler suggested that the volatile components analysed by the AMS were not only water soluble, but also representative of the total organic carbon. This result is particularly interesting, and combined with the unimodal structure of the size distributions provided by the AMS, we hypothesise that the sub-micron aerosol are an internal inorganic/organic mixture. Recent laboratory work has shown that the ion fragmentation patterns of di-carboxylic, humic and fulvic acids in the AMS are all dominated by CO_2^+ and this was the most prevalent organic fragment signal in the ambient measurements throughout the ACE ASIA study. The analysis of the organic functional groups from the impactor samples using the technique of Decesari et al. (2000a) also shows that the carboxylic acids and humic like substances dominate the WSOC fraction of the sub-micron aerosol.

Acknowledgements

This work was supported by the following grants: NER/A/S/2000/00442, NER/S/A/2000/03653 JDA, NER/S/A/2001/06423 DT and NERC GR3/12499. We would like to thank Axel Berner for providing the use of active cloud water collectors and Berner impactors.

References

Allan, J.D., Jimenez, J.L., Coe, H., Bower, K.N., Williams, P.I., Canagaranta, M.R., Jayne, J.T., Worsnop, D.R., 2003a. Quantitative sampling using an aerodyne aerosol mass spectrometer. Part 1: Techniques of data interpretation and error analysis. Journal of Geophysical Research. 108 (D3), 4090.

Allan, J.D., Coe, H., Bower, K.N., Williams, P.I., Gallagher, M.W., Alfarra, M.R., Jimenez, J.L., Nemitz, E., McDonald,

A.G., Canagaratna, M.R., Jayne, J.T., Worsnop, D.R., 2003b. Quantitative sampling using an aerodyne aerosol mass spectrometer. Part 2: Measurements of fine particulate chemical composition in two UK cities. Journal of Geophysical Research. 108 (D3), 4091.

Arimoto, R., Duce, R.A., Savoie, D.L., Prospero, J.M., Talbot, R., Cullen, J.D., Tomza, U., Lewis, N.F., Ray, B.J., 1996. Relationships among aerosol consituents from Asia and the North Pacific during PEM-West A. Journal of Geophysical Research. 101 (D1), 2011–2023.

Bahreini, R., Jimenez, J.L., Wang, J., Flagan, R.C., Seinfeld, J.H., Jayne, J.T., Worsnop, D.R., 2003. Aircraft-based aerosol size and composition measurements during ACE-Asia using an aerodyne aerosol mass spectrometer. Journal of Geophysical Research-Atmospheres 108 (D23), doi:10.1029/2002JD003226, 8645.

Berner, A., Lurzer, C., 1980. Mass size distributions of traffic aerosols at Vienna. Journal of Physical Chemistry 84, 2079–2083.

Carmichael, G.R, Zhang, Y., Chen, L.-L., Hong, M.-S., Ueda, H., 1996. Seasonal variation on aerosol composition at Cheju Island, Korea. Atmospheric Environment 30, 2407–2416.

Carmichael, G.R., Hong, M.-S., Ueda, H., Chen, L.-L., Murano, K., Park, J.K., Lee, Y., Kang, C., Shim, S., 1997. Aerosol composition at Cheju Island, Korea. Journal of Geophysical Research 102 D5, 6047–6061.

Chameides, W.L., Stelson, A.W., 1992. Aqueous-phase chemical processes in deliquescent sea-salt aerosols: a mechanism that couples the atmospheric cycles of S and sea salt. Journal of Geophysical Research 97 (D18), 20565–20580.

Chen, L.-L., Carmichael, G.R., Hong, M.-S., Ueda, H., Shim, S., Song, C.H., Kim, Y.P., Arimoto, R., Prospero, J., Savoie, D., Murano, K., Park, J.K., Lee, H.-G., Kang, C., 1997. Influence of continental outflows on the aerosol composition at Cheju Island, South Korea. Journal of Geophysical Research 102 (D23), 28551–28574.

Decesari, S., Facchini, M.C., Fuzzi, S., Tagliavini, E., 2000a. Characterisation of water-soluble organic compounds in atmospheric aerosol: a new approach. Journal of Geophysical Research 105 (D1), 1481–1489.

Decesari, S., Facchini, M.C., Matta, E., Mircea, M., Fuzzi, S., Putaud, J.P., 2000b. Organic and inorganic solutes in atmospheric aerosol: a full characterization approach. Proceedings from the EUROTRAC Symposium 2000, 27–31 March 2000, Garmisch-Partenkirchen, Germany.

Dentener, F.J., Carmichael, G.R., Zhang, Y., Lelieveld, J., Crutzen, P.J., 1996. Role of mineral aerosol as a reactive surface in the global troposphere. Journal of Geophysical Research 101 (D17), 22869–22889.

Draxler, R.R., Rolph, G.D., 2003. HYSPLIT (Hybrid Single-Particle Lagrangian Integrated Trajectory) Model access via NOAA ARL READY Website (http://www.arl.noaa.gov/ready/hysplit4.html).NOAA Air Resources Laboratory, Silver Spring, MD.

Fan, X.-B., Okada, K., Niimura, N., Kai, K., Arao, K., Shi, G.-Y., Qin, Y., Mitsuta, Y., 1996. Mineral particles collected in China and Japan during the same Asian dust-storm event. Atmospheric Environment 30, 347–351.

Hanisch, F., Crowley, J.N., 2001a. Heterogeneous reactivity of gaseous nitric acid on Al_2O_3, $CaCO_3$, and atmospheric dust samples: A Knudsen cell study. Journal of Physical Chemistry (A) 105, 3096–3106.

Hanisch, F., Crowley, J.N., 2001b. The heterogeneous reactivity of gaseous nitric acid on authentic mineral dust samples, and on individual mineral and clay mineral components. Physical Chemistry Chemical Physics 3, 2474–2482.

Jacobson, M.C., Hansson, H.-C., Noone, K.J., Charlson, R.J., 2000. Organic atmospheric aerosols: review and state of the science. Reviews of Geophysics 38, 267–294.

Jimenez, J.L., Jayne, J.T., Shi, Q., Kolb, C.E., Worsnop, D.R., Yourshaw, I., Seinfeld, J.H., Flagan, R.C., Zhang, X., Smith, K.A., Morris, J., Davidovits, P., 2002. Ambient aerosol sampling with an aerosol mass spectrometer. Journal of Geophysical Research-Atmospheres 108 (D7), doi:10.1029/2001JD001213, 8425.

Kim, Y.P., Moon, K.-C., Shim, S.-G., Lee, J.H., Kim, J.Y., Fung, K., Carmichael, G.R., Song, C.H., Kang, C.H., Kim, H.-K., Lee, C.B., 2000. Carbonaceous species in fine particles at the background sites in Korea between 1994 and 1999. Atmospheric Environment 34, 5053–5060.

Kim, K.-H., Lee, M., Lee, G., Kim, Y.P., Youn, Y.-H., Oh, J.-M., 2002. Observations of aerosol-bound ionic compositions at Cheju Island Korea. Chemosphere 48, 317–327.

Krivacsy, Z., Hoffer, A., Sarvari, Zs., Temesi, D., Baltensperger, U., Nyeki, S., Weingartner, E., Kleefeld, S., Jennings, S.G., 2001. Role of organic and black carbon in the chemical composition of atmospheric aerosol at European background sites. Atmospheric Environment 35, 6231–6244.

Luria, M., Sievering, H., 1991. Heterogeneous and homogeneous oxidation of SO_2 in the remote marine atmosphere. Atmospheric Environment 24, 1489–1496.

Mader, B.T., Schauer, J.J., Seinfeld, J.H., Flagan, R.C., Yu, J.Z., Yang, H., Lim, H.J., Turpin, B.J., DeMinter, J.T., Heidemann, G., Bae, M.S., Quinn, P., Bates, T., Eatough, D.J., Hubert, B.J., Howell, S., 2003. Sampling methods used for the collection of particle-phase organic and elemental carbon during ACE-Asia. Atmospheric Environment 37, 1435–1449.

Matsumoto, K., Nagao, I., Tanaka, H., Miyaji, H., Iida, T., Ikebe, Y., 1998. Seasonal characteristics of organic and inorganic species and their size distributions in atmospheric aerosols over the northwest Pacific Ocean. Atmospheric Environment 32, 1931–1946.

Matta, E., Facchini, M.C., Decesari, S., Mircea, M., Fuzzi, S., Putaud, J.-P., 2001. Size-segregated Organic and Inorganic Composition of Aerosol Samples Collected in a Polluted Area. Proceedings of the 8th European Symposium on the Physico-Chemical Behaviour of Atmospheric Pollutants, 17–20 September 2001, Torino, A Changing Atmosphere. http://ies.jrc.cec.eu.int/Units/cc/events/torino2001/torinocd/Documents/Urban/UP22.htm

Mukai, H., Ambe, Y., Shibata, K., Muku, T., Takeshita, K., Fukuma, T., Takahashi, J., Mizota, S., 1990. Long-term variation of chemical composition of atmospheric aerosol on the Oki Islands in the sea of Japan. Atmospheric Environment 24A, 1379–1390.

Nishikawa, M., 1993. Environmental effects of Kosa aerosol. Journal of Environmental Chemistry 3 (4), 673–682.

Savoie, D.L., Prospero, J.M., 1994. Non-sea-salt sulphate and methanesulphonate at American Samoa. Journal of Geophysical Research. 99 D2, 3587–3596.

Savoie, D.L., Prospero, J.M., 1989a. Comparison of oceanic and continental sources of non-sea-salt sulphate over the Pacific Ocean. Nature 339, 685–687.

Savoie, D.L., Prospero, J.M., 1989b. Effect of continental sources on nitrate concentrations over the Pacific Ocean. Nature 339, 687–689.

Saxena, P., Hildemann, L.M., 1996. Water-soluble organics in atmospheric particles: a critical review of the literature and application of thermodynamics to identify candidate compounds. Journal of Atmospheric Chemistry 24, 57–109.

Sievering, H., Boatman, J., Galloway, J., Keene, W., Kim, Y., Luria, M., Ray, J., 1991. Heterogeneous sulphur conversion in sea-salt aerosol particles: the role of aerosol water content and size distribution. Atmospheric Environment 25A, 1479–1487.

Song, C.H., Carmichael, G.R., 1999. The aging process of naturally emitted aerosol (sea-salt and mineral aerosol) during long-range transport. Atmospheric Environment 33, 2203–2218.

Xuan, J., Sokolik, I.N., 2002. Characterisation of sources and emission rates of mineral dust in northern China. Atmospheric Environment 36, 4863–4876.

Zappoli, S., Andracchio, A., Fuzzi, S., Facchini, M.C., Gelencser, A., Kiss, G., Krivacsy, Z., Molnar, A., Meszaros, E., Hansson, H.-C., Rosman, K., Zebuhr, Y., 1999. Inorganic, organic and macromolecular components of fine aerosol in different areas of Europe in relation to their water solubility. Atmospheric Environment 33, 2733–2743.

Zhang, D., Iwasaka, Y., 1999. Nitrate and sulphate in individual Asian dust–storm particles over Beijing, China in spring of 1995 and 1996. Atmospheric Environment 33, 3213–3223.